On Safe Motion along Artificial Potential Fields

Tuesday 8th April, 2025

Motivation - Navigation and control

Motion Planning → sub-domain of robotics and of general interest in a wide variety of research and practical areas [Mou13; Li03; Gon15]

- autonomous vehicles
- medical domain/ food delivery
- tracking and surveillance (e.g., agriculture)

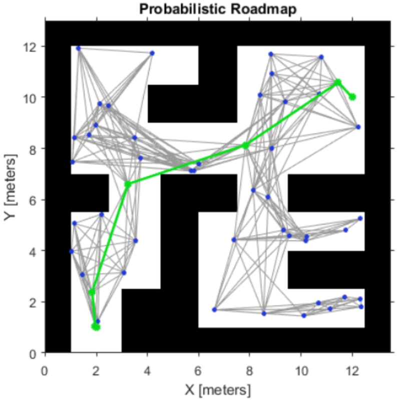

Key factors:

- mission (from where to where?)
- navigation strategy (how?)
- environment (wherein?)

Challenges:

- complexity
- completeness
- reliability

Motivation - Navigation and control

State-of-the-art methods:

- heuristic [LaV06; Wei17] → **sampled/ (graph)-based**
- (constrained) optimization-based [Jan17; Szm17]

Optimization-based methods:

- direct [Ric05; Bal18]
- **indirect** [Fil18; Vla18]

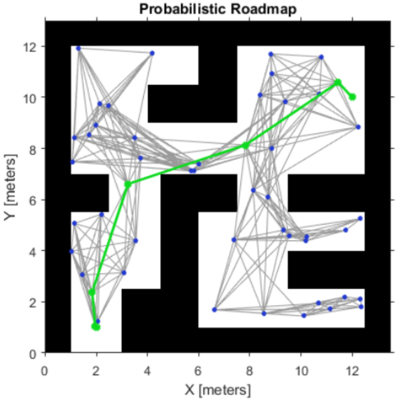

Key factors:

- mission (from where to where?)
- navigation strategy (how?)
- environment (wherein?)

Challenges:

- complexity
- completeness
- reliability

Motivation - Navigation and control

State-of-the-art methods:

- heuristic [LaV06; Wei17] → sampled/ (graph)-based
- (constrained) optimization-based [Jan17; Szm17]

Optimization-based methods:

- direct [Ric05; Bal18]
- **indirect** [Fil18; Vla18]

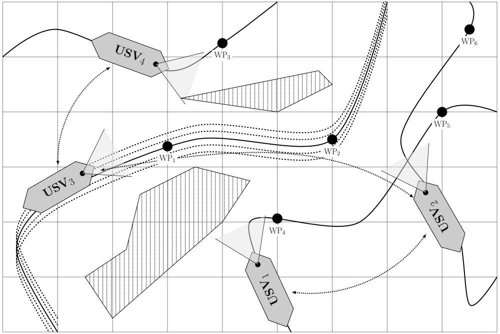

Key factors:

- mission (from where to where?)
- navigation strategy (how?)
- environment (wherein?)

Challenges:

- complexity
- completeness
- reliability

Artificial Potential Field - the idea

Potential field (PF) methods[a] share characteristics from:

- constrained optimization: the control action is the result of minimizing a cost;
- heuristic methods: constraint breaking is penalized, not explicitly enforced.

If the environment is known, the PF may be pre-computed, reducing the runtime effort (e.g., if control action$=\nabla$ PF, the agent moves along the path of minimum resistance)

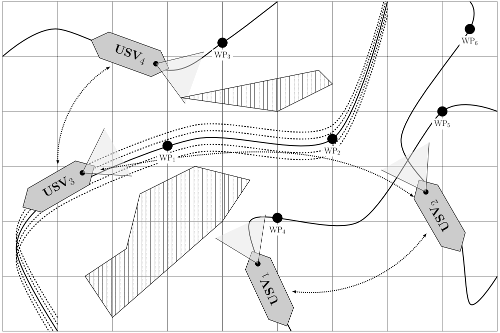

[a] O. Khatib, "Real-time obstacle avoidance for manipulators and mobile robots," in Autonomous robot vehicles, Springer, 1986, pp. 396–404.

Limitations

- the control action may break saturation/rate constraints;
- stalling in local extreme points/infeasibility are possible;
- the obstacles' shape is often ignored (the repulsive PF is radial wrt the center of the obstacle).

Artificial Potential Field - the idea

Potential field (PF) methods[a] share characteristics from:

- constrained optimization: the control action is the result of minimizing a cost;
- heuristic methods: constraint breaking is penalized, not explicitly enforced.

If the environment is known, the PF may be pre-computed, reducing the runtime effort (e.g., if control action=∇ PF, the agent moves along the path of minimum resistance)

[a] O. Khatib, "Real-time obstacle avoidance for manipulators and mobile robots," in Autonomous robot vehicles, Springer, 1986, pp. 396–404.

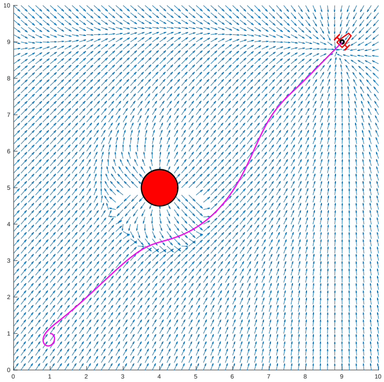

Limitations

- the control action may break saturation/rate constraints;
- stalling in local extreme points/infeasibility are possible;
- the obstacles' shape is often ignored (the repulsive PF is radial wrt the center of the obstacle).

Artificial Potential Field - the idea

Potential field (PF) methods[a] share characteristics from:

- constrained optimization: the control action is the result of minimizing a cost;
- heuristic methods: constraint breaking is penalized, not explicitly enforced.

If the environment is known, the PF may be pre-computed, reducing the runtime effort (e.g., if control action=∇ PF, the agent moves along the path of minimum resistance)

[a] O. Khatib, "Real-time obstacle avoidance for manipulators and mobile robots," in Autonomous robot vehicles, Springer, 1986, pp. 396–404.

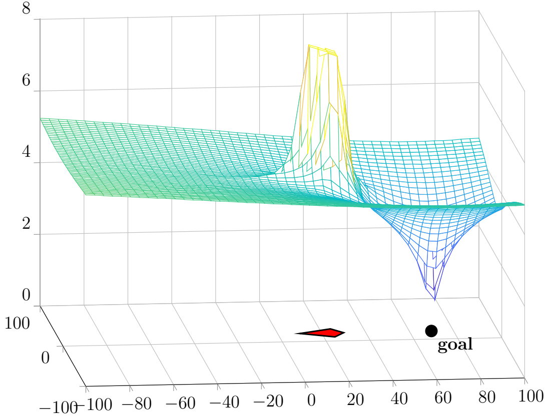

A natural question

How can we adapt *well-established* PF methods for the **polyhedral framework**?

Outline

1. APF - From sphere world to polyhedral world
   - Preliminaries
   - Using sum functions to construct a navigation function
   - Illustrative example

2. Safe Motion Along Harmonic Potential Surfaces
   - Harmonic Potential function
   - Cardinal B-splines
   - Using a B-spline curve as boundary condition
   - Obstacle avoidance implementation

Outline

The Navigation Function – prerequisites

$\varphi : \mathcal{F} \mapsto [0,1]$ is a **navigation function** if it is:

- analytic on $\mathcal{F}$;
- polar on $\mathcal{F}$, with minimum at $q_d \in \operatorname{int}\mathcal{F}$;
- Morse on $\mathcal{F}$;
- admissible on $\mathcal{F}$, i.e., $\partial\mathcal{F} = \varphi^{-1}(0)$.

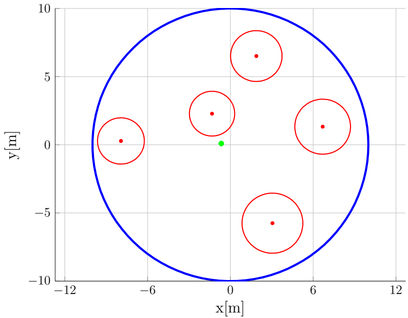

Initial layout:

- sphere world defined by its radius $\rho_0 > 0$ embedded in $\mathbb{R}^n$: $\mathcal{W} = \{q \in \mathbb{R}^n : \|q\| \leq \rho_0\}$;
- a destination $q_d \in \operatorname{int}\mathcal{F}$;
- a collection of non-overlapping M spherical obstacles defined by their centers q_i and radii ρ_i, for $i = 1, \ldots, M$:

$$\mathcal{O}_i = \{q \in \mathbb{R}^n : \|q - q_i\| \leq \rho_i\}.$$

Sphere world example

- repulsive components (world boundary and obstacles)
- attractive component (towards the goal)
- overall navigation function

$$\varphi = \left(\frac{\gamma_d^k}{\gamma_d^k + \beta}\right)^{\frac{1}{k}} = \frac{\gamma_d}{\left(\gamma_d^k + \beta\right)^{\frac{1}{k}}}$$

$$\gamma_d = \|q - q_d\|^2,$$

$$\beta = \prod_{i=0}^{M} \beta_i, \text{ with } \begin{cases} \beta_0 & = \rho_0^2 - \|q\|^2, \\ \beta_i & = \|q - q_i\|^2 - \rho_i^2 \end{cases}$$

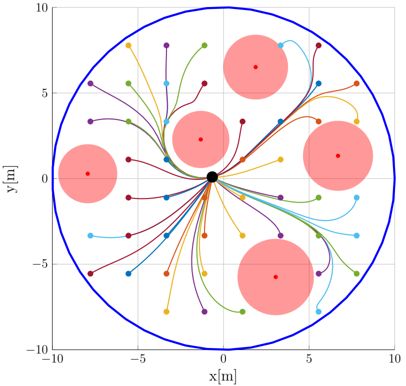

Key issue: the computation of the k which ensures that only a local minimum exists (at the destination)!

The use of spheres has some problems:

- radial repulsive components
- numerical difficulties for obtaining k

Remark

[Kod90] explain in detail how parameters k and ϵ should be chosen and what are the bounds which constrain them for sphere world.

Sphere world example

- repulsive components (world boundary and obstacles)
- attractive component (towards the goal)
- overall navigation function

$$\varphi = \left(\frac{\gamma_d^k}{\gamma_d^k + \beta}\right)^{\frac{1}{k}} = \frac{\gamma_d}{\left(\gamma_d^k + \beta\right)^{\frac{1}{k}}}$$

$$\gamma_d = \|q - q_d\|^2,$$

$$\beta = \prod_{i=0}^{M} \beta_i, \text{ with } \begin{cases} \beta_0 & = \rho_0^2 - \|q\|^2, \\ \beta_i & = \|q - q_i\|^2 - \rho_i^2 \end{cases}$$

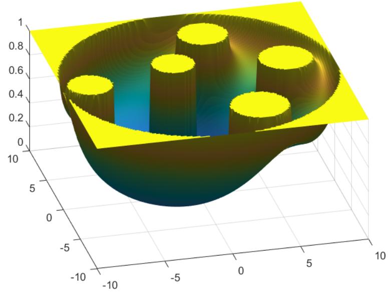

Key issue: the computation of the k which ensures that only a local minimum exists (at the destination)!

The use of spheres has some problems:

- radial repulsive components
- numerical difficulties for obtaining k

Remark

[Kod90] explain in detail how parameters k and ϵ should be chosen and what are the bounds which constrain them for sphere world.

The link towards polyhedral obstacles

- radial repulsive components $\longrightarrow$ work well only for spherical obstacles
- polyhedral obstacles $\longrightarrow$ model various multiple shapes in the environment (any convex set, with arbitrary precision)
- the sum function may be used to characterize closeness to the obstacle
- not least, computations have the potential to be simpler!

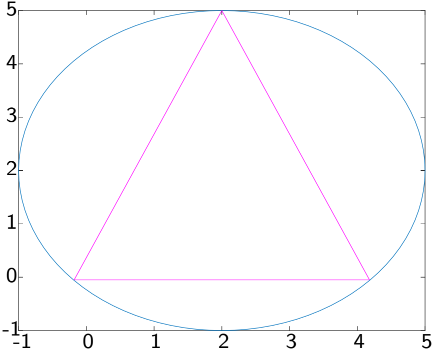

a triangle is not well-penalized by a radial repulsive term

Polyhedral sets

Half-space representation

$$X = \{x \in \mathbb{R}^d : a_i^\top x \leq b_i, i = 1 \dots n_h\},$$

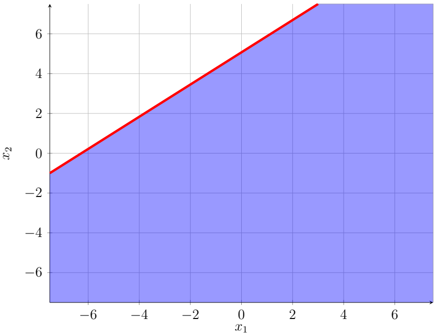

Vertex representation

$$X = \{x \in \mathbb{R}^d : x = \sum_{j=1}^{n_v} \alpha_j v_j, \sum_{j=1}^{n_v} \alpha_j = 1, \alpha_j \geq 0\}.$$

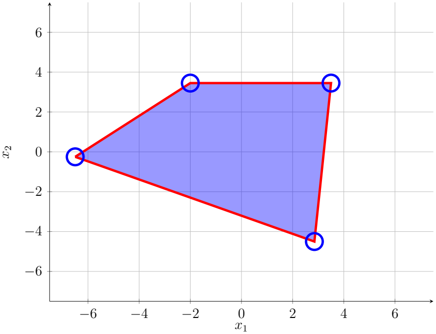

Sum function description

Idea

Using the **sum function** allows to penalize the distance from the obstacle:

$$\beta(P,q) = \begin{cases} 0, & \forall q \in P, \\ > 0, & \text{otherwise.} \end{cases}$$

- Standard sum function[Bor04; Nic22; Sto22]

$$\beta(P,q) = \sum_{j=1}^{N} (a_j^\top q - b_j + |a_j^\top q - b_j|)$$

- Smooth sigmoid approximation

$$\delta_d(q) : \mathbb{R} \mapsto [-1,1], \quad \delta_d(q) = \frac{e^{dq} - e^{-dq}}{e^{dq} + e^{-dq}}$$

- Smooth sum function

$$\beta_d(P,q) = \sum_{j=1}^{N} \left(a_j^\top q - b_j\right) \left[1 + \delta_d\left(a_j^\top q - b_j\right)\right]$$

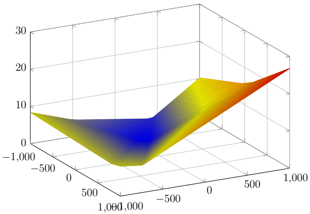

$\beta(P,q)$ example

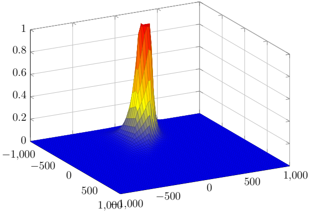

$\frac{c_1}{c_2+\beta(P,q)}$ repulsive component

Obstacle description with a common halfspace seed

- the sum function may be applied repeatedly for any polyhedral obstacle
- here, we consider that all obstacles $\{P_i\}_{i=1:M}$ are described by a common 'seed' list of half-spaces which differ only through their offsets

$$P_i(q) = \{q \in \mathbb{R}^n : \; a_j^\top q \leq b_j^i, \; j = 1:N\},$$

$$\beta_i(q) = \sum_{j=1}^{N} \left(a_j^\top q - b_j^i\right) \left[1 + \delta_d \left(a_j^\top q - b_j^i\right)\right], \quad i = 1:M.$$

- the world - polyhedral set, defined by the same seed matrix A:
$\mathcal{W} = \left\{q \in \mathbb{R}^n : \; a_j^\top q \leq b_j^0, \; j = 1:N\right\}.$

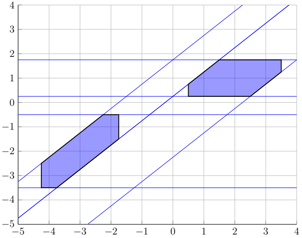

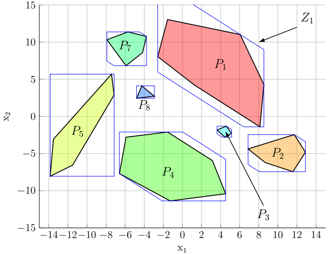

Navigation Function implementation

$$\varphi = \left(\frac{\gamma_d^k}{\gamma_d^k + \beta}\right)^{\frac{1}{k}} = \frac{\gamma_d}{\left(\gamma_d^k + \beta\right)^{\frac{1}{k}}}$$

- Having a critical point $q^\star \Leftrightarrow \nabla\varphi(q^\star) = \nabla\hat{\varphi}(q^\star) = 0$,
- i.e., $k\beta\nabla\gamma_d = \gamma_d\nabla\beta$.

- With condition (based on [Kod90])

$$k\frac{\nabla\gamma_d}{\gamma_d} \neq \sum_{i=0}^{M}\frac{\nabla\beta_i}{\beta_i}, \quad \forall q \in \mathcal{F}_2(\epsilon)$$

there is no critical point (of zero gradient) "far" from the target, the obstacles' and the world's boundaries

- $\mathcal{F}_2(\epsilon) := \mathcal{W} \setminus \left(\{q_d\} \cup \bigcup_{i=0}^{M}\mathcal{B}_i\right)$ - *free space*

Proposition

A sufficient condition, in the polyhedral case, is to verify

$$k \geq N(\epsilon) = \frac{1}{\epsilon} \cdot \max_{\ell=1,\dots,N} \frac{a_\ell^\top \overline{\gamma}_d}{b_\ell^0 - a_\ell^\top q_d}\left(\sum_{j=1}^{N}|a_j|\left[2(M+1) + \lambda\sum_{i=0}^{M}\left|b_j^0 - b_j^i\right|\right]\right)$$

where $\overline{\gamma}_d = 2\max_{q\in\mathcal{W}}\gamma_d(q)$ and λ is given by the sigmoid bounds

Sigmoid bounds

To bound the sum function and its derivatives we need to understand/get the sigmoid bounds:

$$\delta_d'(q) = \frac{4d}{(e^{dq} + e^{-dq})^2},$$

$$\delta_d''(q) = \frac{-8d^2(e^{dq} - e^{-dq})}{(e^{dq} + e^{-dq})^3},$$

$$\delta_d'''(q) = \frac{16d^3(e^{2dq} + e^{-2dq} - 4)}{(e^{dq} + e^{-dq})^4}.$$

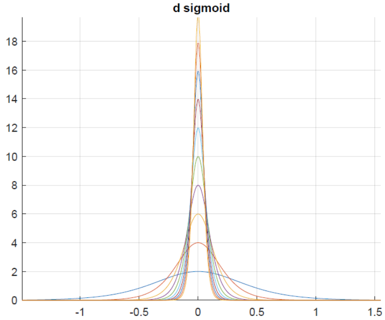

The bounds are given by

$$|\delta_d'(q)| \leq \bar{\delta}_d', \text{ with } \bar{\delta}_d' := \delta_d'(0) = \lambda.$$

$$|\delta_d''(q)| \leq \bar{\delta}_d'', \text{ with } \bar{\delta}_d'' := |\delta_d''(q_\pm^\star)| = \frac{4\sqrt{3}}{9}\lambda^2.$$

Bounds for the smooth sum functions

- Bounds for the gradient

$$\nabla\beta_i(q) = \sum_{j=1}^{N} a_j \left[(1+\delta_d(\cdot)) + \left(a_j^\top q - b_j^i\right)\delta_d'(\cdot)\right] \quad \implies \quad |\nabla\beta_i(q)| \leq \sum_{j=1}^{N} |a_j| \left[2 + \left|b_j^0 - b_j^i\right|\lambda\right]$$

- Bounds for the Hessian

$$\nabla^2\beta_i(q) = \sum_{j=1}^{N} a_j a_j^\top \cdot \left[2\delta_d'(\cdot) + \left(a_j^\top q - b_j^i\right)\delta_d''(\cdot)\right] \quad \implies \quad |\nabla^2\beta_i(q)| \leq \sum_{j=1}^{N} \left|a_j a_j^\top\right| \cdot \left[2\lambda + \left|b_j^0 - b_j^i\right| \frac{4\sqrt{3}}{9}\lambda^2\right].$$

- useful to analyze the bounds for the scaling factor ϵ and implicitly of k

Illustrative Example – 1/2

- single integrator dynamics $\rightarrow \dot{q}(t) = u(t)$
- $u(t) = -\nabla\varphi(q(t))$
- 3 obstacles for illustration purpose:

$$A = \begin{bmatrix} -0.12 & -0.16 \\ 0.11 & -0.09 \\ 0.07 & 0.07 \\ -0.35 & 0.13 \end{bmatrix}, \quad \{b^i\} \in \left\{ \begin{bmatrix} 0.01 \\ 0.13 \\ 0.07 \\ -0.22 \\ 0.95 \end{bmatrix}, \begin{bmatrix} 0.16 \\ -0.14 \\ 0.09 \\ 0.63 \\ 1.25 \end{bmatrix}, \begin{bmatrix} 0.16 \\ 0.08 \\ -0.06 \\ -0.24 \\ 0.05 \end{bmatrix} \right\} \text{with } i = 1:3.$$

- $q_d = \begin{bmatrix} 0 & 0.5 \end{bmatrix}^\top$

Illustrative Example – 2/2

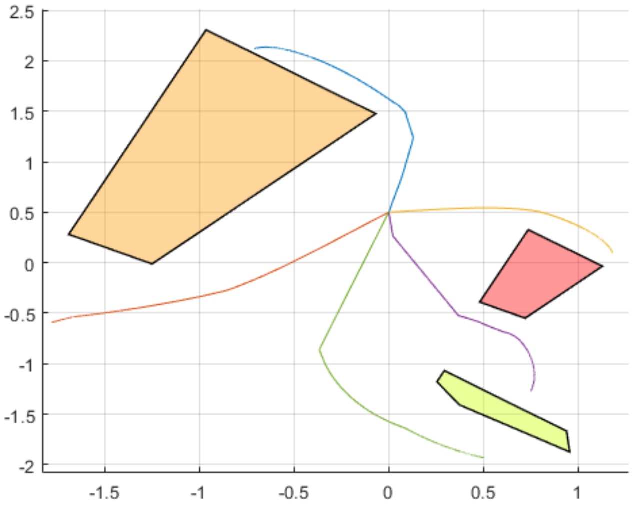

Outline

1. APF - From sphere world to polyhedral world
2. Safe Motion Along Harmonic Potential Surfaces
   - Harmonic Potential function
   - Cardinal B-splines
   - Using a B-spline curve as boundary condition
   - Obstacle avoidance implementation

General idea

- a finite number of non-overlapping regions :

  $\mathbb{O} = \bigcup_{j=1}^{N_o} \mathcal{O}_j;\ \mathrm{int}(\mathcal{O}_i) \cap \mathrm{int}(\mathcal{O}_j) = \emptyset, \forall i \neq j$

- a feasible domain (*free space*) : $\mathcal{C}_{\mathbb{X}}(\mathbb{O}) \triangleq \mathbb{X} \setminus \mathbb{O}$

- we can decompose the *free space* into a collection of cells $\to$ *polyhedral complex* [Fuk20]:

$$\mathcal{C}_{\mathbb{X}}(\mathbb{O}) = \bigcup_{\ell=1}^{N_c} P_\ell;$$

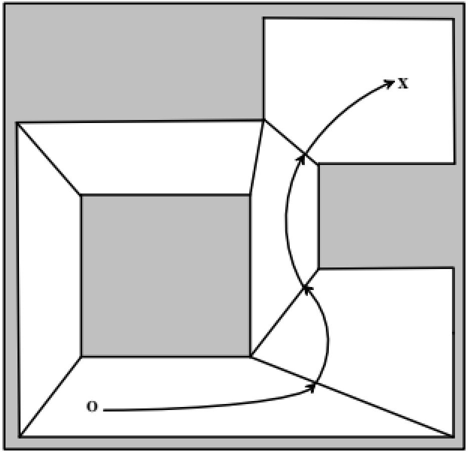

Idea

Forcing the agent's trajectories to pass through a pre-computed sequence of regions $\{P_{\ell_1} \mapsto P_{\ell_2} \mapsto \dots\}$ the agent **avoids the obstacles and arrives at the destination**.

General idea

- a finite number of non-overlapping regions :

  $\mathbb{O} = \bigcup_{j=1}^{N_o} \mathcal{O}_j;\ \text{int}(\mathcal{O}_i) \cap \text{int}(\mathcal{O}_j) = \emptyset, \forall i \neq j$

- a feasible domain (*free space*) : $\mathcal{C}_{\mathbb{X}}(\mathbb{O}) \triangleq \mathbb{X} \setminus \mathbb{O}$

- we can decompose the *free space* into a collection of cells $\rightarrow$ *polyhedral complex* [Fuk20]:

$$\mathcal{C}_{\mathbb{X}}(\mathbb{O}) = \bigcup_{\ell=1}^{N_c} P_\ell;$$

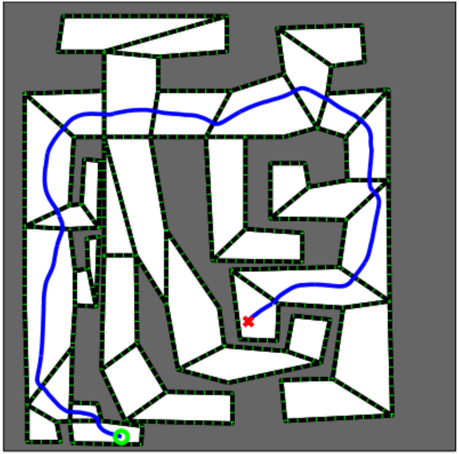

Idea

Forcing the agent's trajectories to pass through a pre-computed sequence of regions $\{P_{\ell_1} \mapsto P_{\ell_2} \mapsto \dots\}$ the agent **avoids the obstacles and arrives at the destination**.

How can we force $\{P_{\ell_1} \mapsto P_{\ell_2} \mapsto \dots\}$?

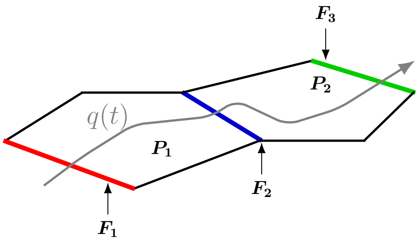

Idea

With each cell we associate an *individual control policy* designed such that they will cause any configuration within the cell to move along a trajectory into a specified adjacent target cell specified by the partial order.

- during the evolution of the system trajectory, the configuration will not exit other than by crossing the common boundary
- each cell is free of obstacles $\rightarrow$ we can design a **potential field** over the model space that is free of local minima.

How can we force $\{P_{\ell_1} \mapsto P_{\ell_2} \mapsto \dots\}$?

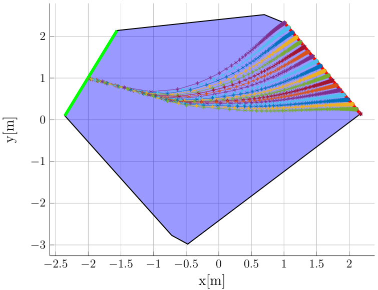

Idea

With each cell we associate an *individual control policy* designed such that they will cause any configuration within the cell to move along a trajectory into a specified adjacent target cell specified by the partial order.

- during the evolution of the system trajectory, the configuration will not exit other than by crossing the common boundary
- each cell is free of obstacles $\rightarrow$ we can design a **potential field** over the model space that is free of local minima.

Harmonic Potential function – definitions

- **Laplace's heat equation**:

$$\nabla^2\gamma(x,y) = \frac{\partial^2}{\partial x^2}\gamma + \frac{\partial^2}{\partial y^2}\gamma = 0$$

- $\forall (x,y) \in \operatorname{int}\mathcal{C}$
- $\mathcal{C} \subset \mathbb{R}^2$ - a closed region with non-empty interior

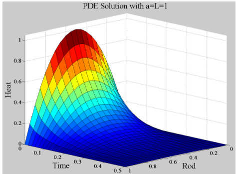

Main Advantage

- $\gamma(x,y)$ has no points of local minima/maxima, $\forall (x,y) \in \operatorname{int}\mathcal{C}$;
- all local minima/maxima of $\gamma(x,y)$ are on the boundary of $\mathcal{C}$.

- the Laplace operator in polar coordinates:

$$\nabla^2 = \frac{\partial^2}{\partial r^2} + \frac{1}{r}\frac{\partial}{\partial r} + \frac{1}{r^2}\frac{\partial^2}{\partial \theta^2}.$$

- let $\mathcal{C} = \mathcal{B} = \{(x,y):\ x^2+y^2 \le 1\} = \{(r,\theta):\ r \le 1, |\theta| \le \pi\}$
- the solution over its boundary $(r=1) \rightarrow$ the "Dirichlet boundary problem" $\gamma(r=1,\theta) = h(\theta)$
- the surface that verifies $\nabla^2\gamma(r,\theta) = 0, \forall (r,\theta) \in \operatorname{int}\mathcal{B}$:

$$\gamma(r,\theta) = A_0 + \sum_{n=1}^{\infty} A_n r^n \cos n\theta + B_n r^n \sin n\theta$$

A_n, B_n from the trigonometric Fourier series of $h(\theta)$

Harmonic Potential function – definitions

- **Laplace's heat equation**:

$$\nabla^2\gamma(x,y) = \frac{\partial^2}{\partial x^2}\gamma + \frac{\partial^2}{\partial y^2}\gamma = 0$$

- $\forall (x,y) \in \operatorname{int} \mathcal{C}$
- $\mathcal{C} \subset \mathbb{R}^2$ - a closed region with non-empty interior

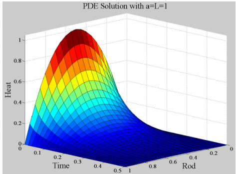

Main Advantage

- $\gamma(x,y)$ has no points of local minima/maxima, $\forall (x,y) \in \operatorname{int} \mathcal{C}$;
- all local minima/maxima of $\gamma(x,y)$ are on the boundary of $\mathcal{C}$.

- the Laplace operator in polar coordinates:

$$\nabla^2 = \frac{\partial^2}{\partial r^2} + \frac{1}{r}\frac{\partial}{\partial r} + \frac{1}{r^2}\frac{\partial^2}{\partial \theta^2}.$$

- let $\mathcal{C} = \mathcal{B} = \{(x,y) : \; x^2 + y^2 \leq 1\} = \{(r,\theta) : \; r \leq 1, |\theta| \leq \pi\}$
- the solution over its boundary ($r = 1$) $\rightarrow$ the "Dirichlet boundary problem" $\gamma(r = 1, \theta) = h(\theta)$
- the surface that verifies $\nabla^2\gamma(r,\theta) = 0, \forall (r,\theta) \in \operatorname{int} \mathcal{B}$:

$$\gamma(r,\theta) = \frac{1}{2\pi}\int_{-\pi}^{\pi} h(\phi)\frac{1 - r^2}{1 - 2\cos(\theta - \phi)r + r^2}\,d\phi.$$

Poisson kernel

Harmonic Potential function – classic implementation 1/2

[Con03]

- $\gamma(r, \theta)$ can be computed over the unit disk, i.e., $\forall(r, \theta) \in \mathcal{B}$
- with boundary conditions

$$h(\theta) = \begin{cases} 0, & \theta \in [\alpha_0, \alpha_1] \\ V, & \text{otherwise} \end{cases},$$

- $-\pi < \alpha_0 < \alpha_1 < \pi$ and apply the Poisson kernel

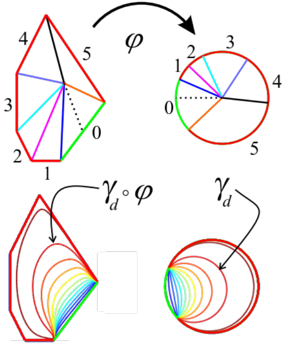

$$\gamma(r, \theta) = \frac{V}{\pi}\left[\arctan\left(\frac{r\sin(\alpha_1 - \theta)}{1 - r\cos(\alpha_1 - \theta)}\right) - \arctan\left(\frac{r\sin(\alpha_0 - \theta)}{1 - r\cos(\alpha_0 - \theta)}\right) + \frac{\alpha_1 - \alpha_0}{2}\right],$$

- an isomorphic mapping $\varphi(\cdot)$: 2D polyhedra $\rightleftharpoons$ disk

Harmonic Potential function – classic implementation 2/2

- an arbitrary/ non-empty polytope:

$$P = \{q \in \mathbb{R}^2 : \beta_i(q) \geq 0, \forall i = 1, \ldots, m\},$$

- with $\beta_i(q) = a_i^\top q - b_i$
- the diffeomorphic mapping:

$$\varphi(q) = \frac{q}{\|q\| + \beta(q)}$$

- by construction:
$q \in P \implies \varphi(q) \in \mathcal{B}$ and $q \in \partial P \implies \varphi(q) \in \partial\mathcal{B}$.

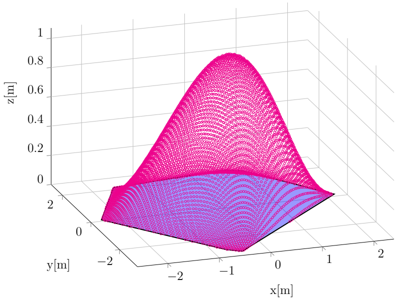

$$\beta(q) = \beta_{\max}^{\frac{1-m}{m}} \prod_{i=1}^{m} \beta_i(q),$$

- mapping $\beta(q)$ over P:

Harmonic Potential function – classic implementation 2/2

- an arbitrary/ non-empty polytope:

$$P = \{q \in \mathbb{R}^2 : \beta_i(q) \geq 0, \forall i = 1, \ldots, m\},$$

- with $\beta_i(q) = a_i^\top q - b_i$
- the diffeomorphic mapping:

$$\varphi(q) = \frac{q}{\|q\| + \beta(q)}$$

- by construction:
  $q \in P \implies \varphi(q) \in \mathcal{B}$ and $q \in \partial P \implies \varphi(q) \in \partial\mathcal{B}$.

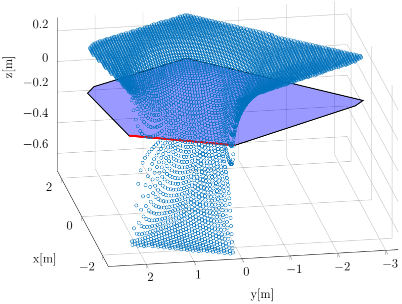

$$\gamma_P(q) := \gamma(\varphi(q)).$$

- harmonic potential surface over P, i.e. $\mathcal{B} \leftarrow\!\shortmid P$

Harmonic Potential function – illustration

By choosing/assuming:

- $[\alpha_0, \alpha_1] = \varphi(\mathcal{F}_{\ell_j})$ where $\mathcal{F}_{\ell_j} = P_{\ell_j} \cap P_{\ell_{j+1}}$
- the control action proportional to the surface gradient (i.e., to follow the paths of minimum resistance).

$$\ddot{q} = u, \; u = K\left(X(q) - \dot{q}\right) + \dot{X}(q)$$

- with $K > 0$ denotes the "velocity regulation" gain

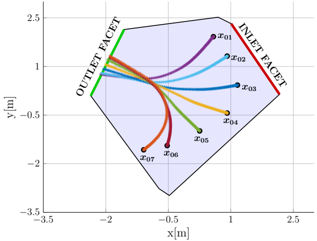

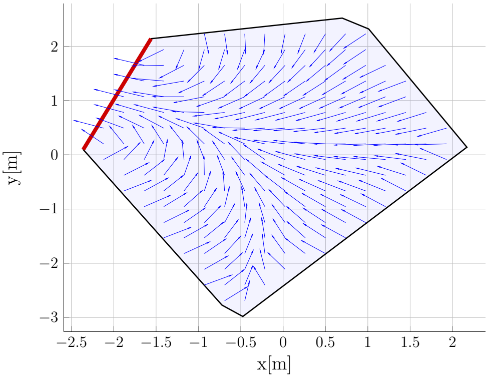

$$X(q) = -\frac{D_q \gamma_P^\top}{\|D_q \gamma_P\|} = -\frac{D_q \varphi^\top D_{\varphi(q)} \gamma^\top}{\|D_q \varphi^\top D_{\varphi(q)} \gamma^\top\|}$$

- the normalized negative gradient

Harmonic Potential function – illustration

By choosing/assuming:

- $[\alpha_0, \alpha_1] = \varphi(\mathcal{F}_{\ell_j})$ where $\mathcal{F}_{\ell_j} = P_{\ell_j} \cap P_{\ell_{j+1}}$
- the control action proportional to the surface gradient (i.e., to follow the paths of minimum resistance).

$$\ddot{q} = u, \; u = K\left(X(q) - \dot{q}\right) + \dot{X}(q)$$

- with $K > 0$ denotes the “velocity regulation” gain

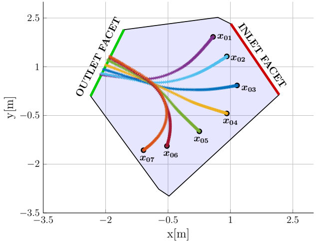

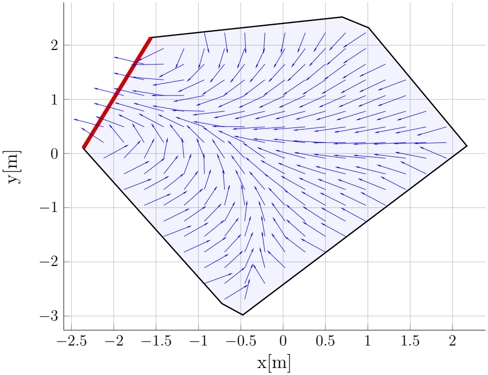

Limitations

The boundary condition imposes sharp gradients near the exit facet. How can we avoid that?

Harmonic Potential function – illustration

By choosing/assuming:

- $[\alpha_0, \alpha_1] = \varphi(\mathcal{F}_{\ell_j})$ where $\mathcal{F}_{\ell_j} = P_{\ell_j} \cap P_{\ell_{j+1}}$
- the control action proportional to the surface gradient (i.e., to follow the paths of minimum resistance).

$$\ddot{q} = u,\ u = K\left(X(q) - \dot{q}\right) + \dot{X}(q)$$

- with $K > 0$ denotes the "velocity regulation" gain

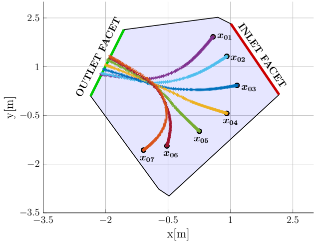

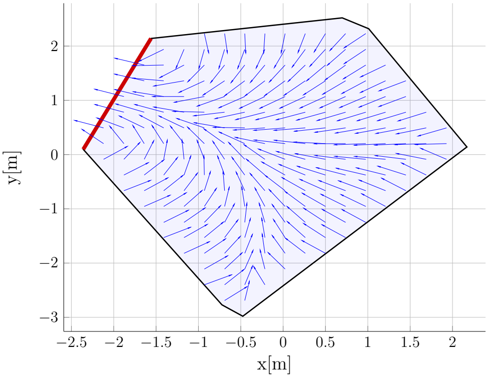

Limitations

The boundary condition imposes sharp gradients near the exit facet. How can we avoid that? → use of **B-Spline curves**

Cardinal B-splines – definition

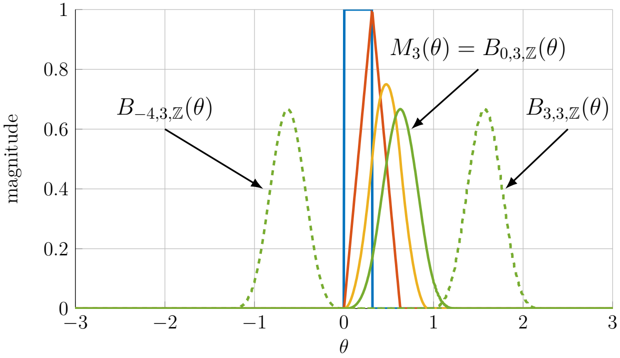

The cardinal splines [Lyc18] of degree $p \geq 1$:

$$B_{k,p,\mathbb{Z}}(t)$$

are obtained from:

$$M_0(\theta) = \begin{cases} 1, & \forall \theta \in [0,1), \\ 0, & \text{otherwise}, \end{cases}$$

$$M_p(\theta) = \frac{\theta}{p} M_{p-1}(\theta) + \frac{p+1-\theta}{p} M_{p-1}(\theta - 1),$$

$$B_{k,p,\mathbb{Z}}(\theta) = B_{0,p,\mathbb{Z}}(\theta - k) := M_p(\theta - k), \quad \forall k \in \mathbb{Z}.$$

Cardinal B-splines – properties

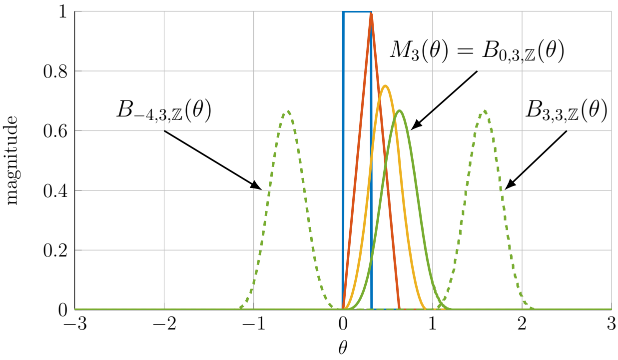

- Local support:

$$B_{k,p,\mathbb{Z}}(\theta) = 0, \forall \theta \notin [k, k+p+1);$$

- Partition of unity:

$$\sum_{k=m-p}^{m} B_{k,p,\mathbb{Z}}(\theta) = 1, \forall \theta \in [m, m+1);$$

- The Fourier transform is given by

$$\mathcal{F}\Big(M_p(\theta)\Big)(\omega) = \left(\frac{1-e^{-j\omega}}{j\omega}\right)^{p+1}.$$

The B-spline curve as a boundary condition

- Cardinal B-spline scaled with an arbitrary $\lambda \in \mathbb{R}_{>0}$:

$$\sigma_k(\theta) = B_{k,p,\mathbb{Z}}\left(\frac{\theta}{\lambda}\right) = M_p\left(\frac{\theta}{\lambda} - k\right),$$

- weighted with control points P_k:

$$h(\theta) = \sum_{k \in \mathcal{K}} P_k \sigma_k(\theta), \quad \forall \theta \in [-\pi, \pi]$$

- its Fourier Transform:

$$H(\omega) = \sum_{k \in \mathcal{K}} P_k \left(\frac{1 - e^{-j\lambda\omega}}{j\lambda\omega}\right)^{p+1} \cdot \lambda e^{-j\lambda\omega k}$$

Idea

By suitable choice of λ and $\mathcal{K}$, $h(\theta)$ of period 2π

Problem

The surface that verifies $\nabla^2\gamma(r,\theta) = 0, \forall(r,\theta) \in \operatorname{int}\mathcal{B}$:

$$\gamma(r,\theta) = A_0 + \sum_{n=1}^{\infty} A_n r^n \cos n\theta + B_n r^n \sin n\theta$$

A_n, B_n from the trigonometric Fourier series of $h(\theta)$

$$A_0 = \frac{\lambda}{2\pi} \sum_{k \in \mathcal{K}} P_k,$$

$$A_n = \frac{(-1)^{\frac{p+1}{2}}}{\pi \lambda^p n^{p+1}} \sum_{k \in \mathcal{K}} P_k \sum_{\ell=0}^{p+1} (-1)^\ell \binom{p+1}{\ell} \cos \lambda n(\ell + k),$$

$$B_n = \frac{(-1)^{\frac{p+1}{2}}}{\pi \lambda^p n^{p+1}} \sum_{k \in \mathcal{K}} P_k \sum_{\ell=0}^{p+1} (-1)^\ell \binom{p+1}{\ell} \sin \lambda n(\ell + k).$$

The B-spline curve as a boundary condition

- Cardinal B-spline scaled with an arbitrary $\lambda \in \mathbb{R}_{>0}$:

$$\sigma_k(\theta) = B_{k,p,\mathbb{Z}}\left(\frac{\theta}{\lambda}\right) = M_p\left(\frac{\theta}{\lambda} - k\right),$$

- weighted with control points P_k:

$$h(\theta) = \sum_{k\in\mathcal{K}} P_k \sigma_k(\theta), \quad \forall\theta \in [-\pi, \pi]$$

- its Fourier Transform:

$$H(\omega) = \sum_{k\in\mathcal{K}} P_k \left(\frac{1 - e^{-j\lambda\omega}}{j\lambda\omega}\right)^{p+1} \cdot \lambda e^{-j\lambda\omega k}$$

Idea

By suitable choice of λ and $\mathcal{K}$, $h(\theta)$ of period 2π

Problem

The surface that verifies $\nabla^2\gamma(r,\theta) = 0, \forall(r,\theta) \in \operatorname{int}\mathcal{B}$:

$$\gamma(r,\theta) = A_0 + \sum_{n=1}^{\infty} A_n r^n \cos n\theta + B_n r^n \sin n\theta$$

A_n, B_n from the trigonometric Fourier series of $h(\theta)$

$$\gamma(r,\theta) = \frac{\lambda}{2\pi}\sum_{k\in\mathcal{K}} P_k + \frac{(-1)^{\frac{p+1}{2}}}{\pi\lambda^p}\sum_{k\in\mathcal{K}} P_k \sum_{\ell=0}^{p+1}(-1)^\ell\binom{p+1}{\ell} \sum_{n\geq 1}\frac{r^n}{n^{p+1}}\cos n\left[\lambda(\ell+k) - \theta\right].$$

Choosing the control points $P_k, k \in \mathcal{K}$

Problem

- $h(\theta) = -1$, $\forall \theta \in [\alpha_0, \alpha_1]$;
- $h(\theta)$ has no local minima **outside** $[\alpha_0, \alpha_1]$.

Proposed solution:

- λ, m such that $\lambda m = \pi$
- $\mathcal{K} = \{-m, \dots, m - p - 1\}$ and

$$P_k = \begin{cases} -1, & \left\lceil \frac{\alpha_0}{\lambda} \right\rceil - p \leq k \leq \left\lfloor \frac{\alpha_1}{\lambda} \right\rfloor, \\ 0, & \text{otherwise.} \end{cases}$$

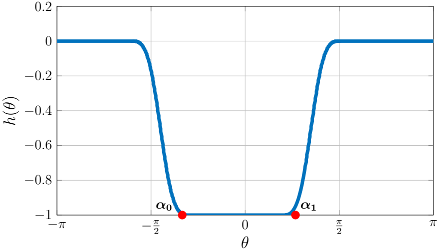

Practical consequences:

- only for $k \in \mathcal{K}$, support of $\sigma_k(\theta)$ is fully inside $[-\pi, \pi]$
- $h(\theta) = -1$ only for

$$\theta \in \left[\lambda \left\lceil \frac{\alpha_0}{\lambda} \right\rceil, \lambda \left\lfloor \frac{\alpha_1}{\lambda} \right\rfloor\right] \subseteq [\alpha_0, \alpha_1],$$

$$\gamma(r, \theta) = -\frac{(\overline{k} - \underline{k})\lambda}{2\pi} - \frac{(-1)^{\frac{p+1}{2}}}{\pi \lambda^p} \operatorname{Re}\left(\sum_{\ell=0}^{p} (-1)^{\ell} \binom{p}{\ell} \left[\mathrm{Li}_{p+1}\left(re^{j[\lambda(\ell+\underline{k})-\theta]}\right) - \mathrm{Li}_{p+1}\left(re^{j[\lambda(\ell+\overline{k})-\theta]}\right)\right]\right).$$

Illustrative example

$$\gamma(r,\theta) = -\frac{(\overline{k}-\underline{k})\lambda}{2\pi} - \frac{(-1)^{\frac{p+1}{2}}}{\pi\lambda^p}\mathrm{Re}\left(\sum_{\ell=0}^{p}(-1)^{\ell}\binom{p}{\ell}\left[\mathrm{Li}_{p+1}\left(re^{j[\lambda(\ell+\underline{k})-\theta]}\right) - \mathrm{Li}_{p+1}\left(re^{j[\lambda(\ell+\overline{k})-\theta]}\right)\right]\right).$$

- $\underline{k} = \left\lceil \frac{\alpha_0}{\lambda} \right\rceil - p$ and $\overline{k} = \left\lfloor \frac{\alpha_1}{\lambda} \right\rfloor - 1$
- $\lambda = \pi/10$, $p = 3$ and $m = 10$
- $\alpha_0 = -\pi/3$ and $\alpha_1 = \pi/6$
- *polylog* [a] functions have been approximated by truncating after the first 15 terms in the sum

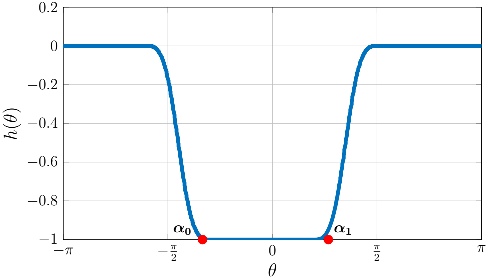

[a] polylogarithm $\mathrm{Li}_{p+1}(z)$ of order $p+1$, also known as the Jonquière's function

$$\mathrm{Li}_{p+1}(z) = \sum_{n=1}^{\infty}\frac{z^n}{n^{p+1}}$$

Illustrative example

$$\gamma(r,\theta) = -\frac{(\overline{k}-\underline{k})\lambda}{2\pi} - \frac{(-1)^{\frac{p+1}{2}}}{\pi\lambda^p}\mathrm{Re}\left(\sum_{\ell=0}^{p}(-1)^\ell\binom{p}{\ell}\left[\mathrm{Li}_{p+1}\left(re^{j[\lambda(\ell+\underline{k})-\theta]}\right)-\mathrm{Li}_{p+1}\left(re^{j[\lambda(\ell+\overline{k})-\theta]}\right)\right]\right).$$

- $\underline{k} = \left\lceil\frac{\alpha_0}{\lambda}\right\rceil - p$ and $\overline{k} = \left\lfloor\frac{\alpha_1}{\lambda}\right\rfloor - 1$
- $\lambda = \pi/10$, $p = 3$ and $m = 10$
- $\alpha_0 = -\pi/3$ and $\alpha_1 = \pi/6$
- *polylog* [a] functions have been approximated by truncating after the first 15 terms in the sum

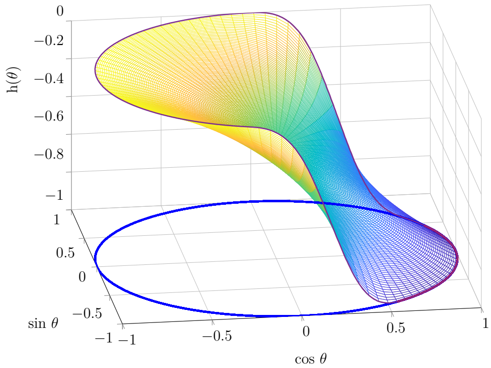

[a] polylogarithm $\mathrm{Li}_{p+1}(z)$ of order $p+1$, also known as the Jonquière's function

$$\mathrm{Li}_{p+1}(z) = \sum_{n=1}^{\infty}\frac{z^n}{n^{p+1}}$$

Obstacle avoidance implementation

- 3 polyhedral obstacles
- 19 support hyperplanes $\rightarrow$ hyperplanes arrangement [Pro16]
- 104 cells describe the feasible space as : $\mathcal{C}_{\mathbb{X}}(\mathbb{O}) = \bigcup_{\ell=1}^{104} P_\ell;$
- the other 12 cells partition the obstacles
- the partitioning is a cell complex

A natural question

How can we identify the pre-computed sequence of regions $\{P_{\ell_1} \mapsto P_{\ell_2} \mapsto \dots\}$?

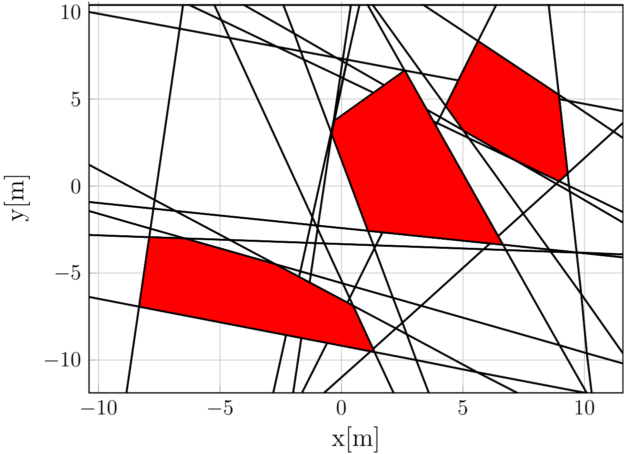

Obstacle avoidance implementation

- 3 polyhedral obstacles
- 19 support hyperplanes → hyperplanes arrangement [Pro16]
- 104 cells describe the feasible space as : $\mathcal{C}_{\mathbb{X}}(\mathbb{O}) = \bigcup_{\ell=1}^{104} P_\ell;$
- the other 12 cells partition the obstacles
- the partitioning is a cell complex

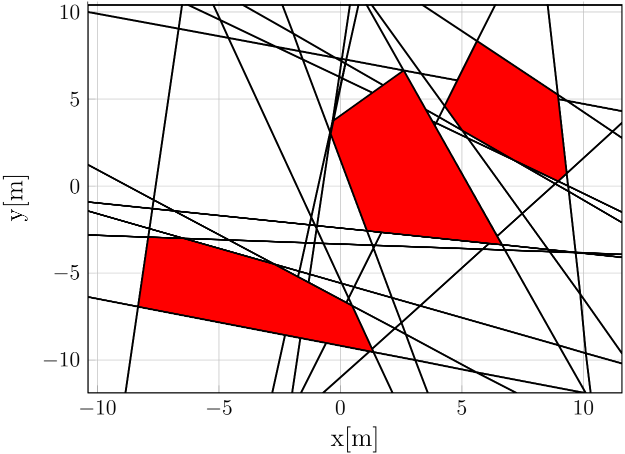

A natural question

How can we identify the pre-computed sequence of regions $\{P_{\ell_1} \mapsto P_{\ell_2} \mapsto \dots\}$?

Solution: construct a “cell-connectivity” graph

Connectivity graph – 1/2

From cell decomposition to a directed graph

Define a digraph $\Gamma = (\mathcal{N}, \mathcal{E})$, based on the cell complex $\{P_\ell\}_{i=1:104}$:

- $\mathcal{N}$- the facets of the partition cells
- for $\mathcal{E}$: two facets are part of the same cell $\rightarrow$ there exists a corresponding graph edge; .
- to each graph edge $\Longrightarrow$ a weight which measures the effort of traveling from the "in" to the "out" facet.

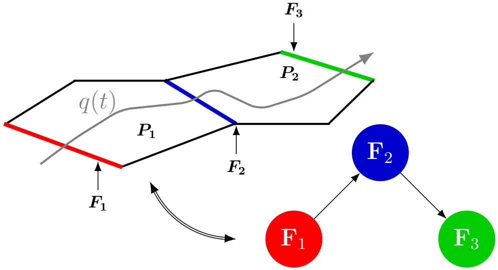

Connectivity graph – 2/2

- 116 cells
- 601 graph nodes (unique cell facets)
- 205 edges
- the nodes that correspond to obstacle facets but also the edges connected to them $\longrightarrow$ infeasible

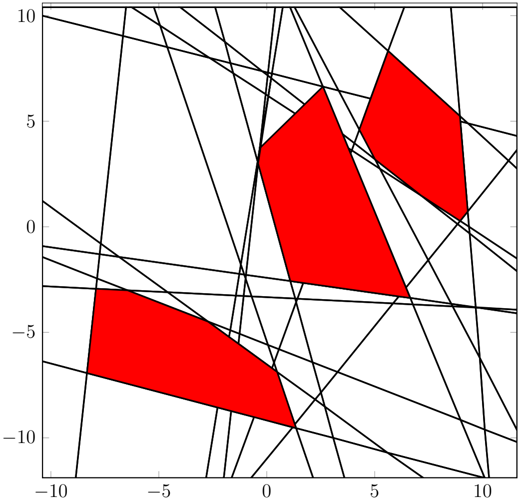

Connectivity graph – 2/2

- 116 cells
- 601 graph nodes (unique cell facets)
- 205 edges
- the nodes that correspond to obstacle facets but also the edges connected to them ⟶ infeasible

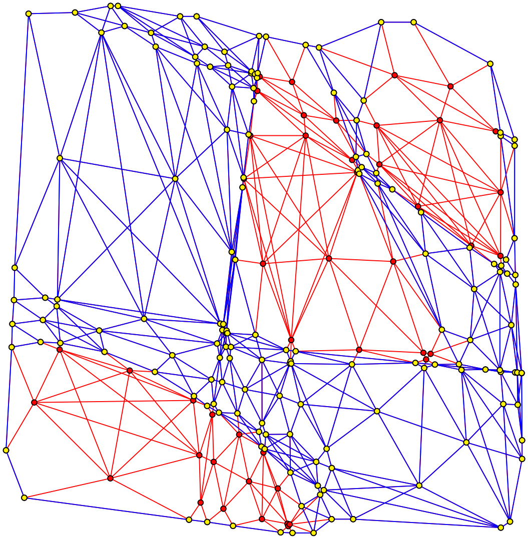

Connectivity graph – 2/2

- 116 cells
- 601 graph nodes (unique cell facets)
- 205 edges
- the nodes that correspond to obstacle facets but also the edges connected to them ⟶ infeasible

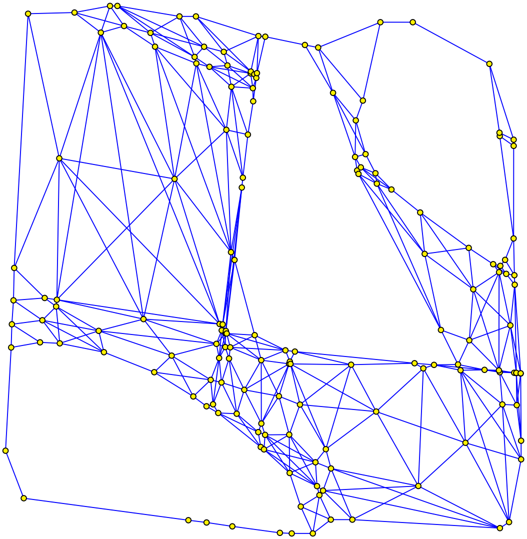

Edge weights alternatives

Having the feasible connectivity graph, we propose 2 approaches to compute the weight of the edge linking nodes i, j:

- path length between the associated "in" and "out" facets

$$w_{\text{length}}(i,j) = \left\{ \int_0^T \|\dot{q}(t)\| dt : \forall q(0) \in F_i \right\},$$

- the control action "spent" when traveling between the "in" and "out" facets

$$w_{\text{action}}(i,j) = \left\{ \int_0^T \|\ddot{q}(t)\| dt : \forall q(0) \in F_i \right\},$$

- $q(0)$ can be anywhere on the "in" $\rightarrow \mathbf{w} = [\underline{w}, \overline{w}] \subset \mathbb{R}$.
- $w_{\text{length}} \in [66.65, 78.91]$, $w_{\text{action}} \in [29.84, 50.52]$

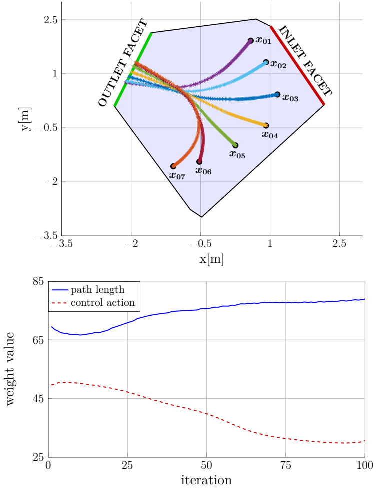

Shortest path criterion alternatives – 1/2

Next step: employ a graph search algorithm[Pal84], e.g. Dijkstra's algorithm [Kar11], **but** $\mathbf{w} = [\underline{w}, \overline{w}] \subset \mathbb{R}$

Multiple options for the criteria of the shortest-path alg.:

- *['max']* the upper bound $\overline{w}$
- *['mid']* $m(\mathbf{w}) = \frac{\underline{w}+\overline{w}}{2}$
- *['interval']* $\mathbf{w} = \langle m(\mathbf{w}), width(\mathbf{w}) \rangle$ along with interval arithmetic [Jau01] for total cost and an adapted alg..

Weight	Variants	Total Cost	n_n
w_{length}	'mid'	151.63	23
	'max'	298.60	25
	'interval'	$[0.98, 302.28]$	23
w_{action}	'mid'	295.44	20
	'max'	460.75	26
	'interval'	$[126.39, 464.17]$	20

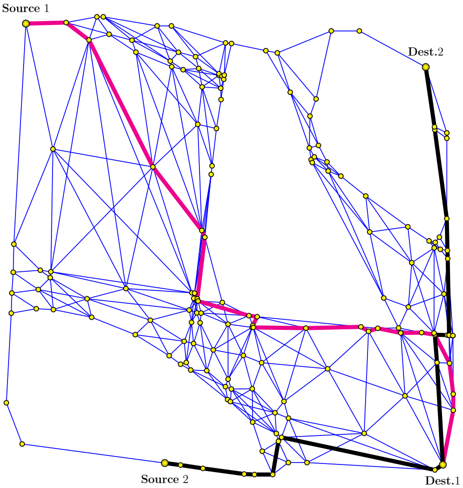

Shortest path criterion alternatives – 2/2

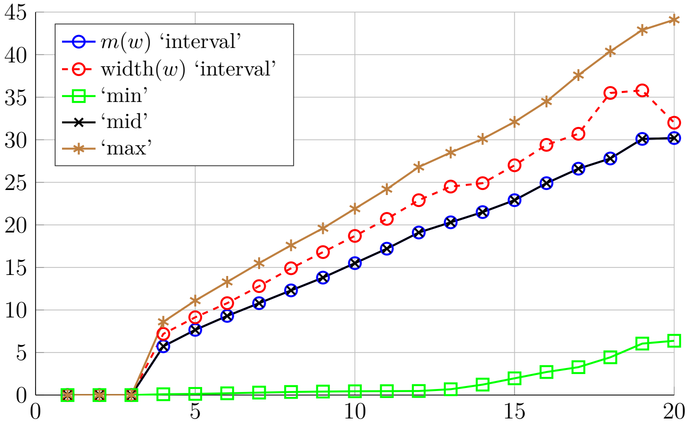

- the total cost when averaged over all pairs of source-target having the same path length.
- a proportional increase in cost, regardless of the specific weight chosen
- mostly, the various methods work in lock-step with small variation
- the outlier is the 'min' weight, BUT not a practical choice – a too-optimistic cost.

References I

[Bal18] C. Bali and A. Richards, "Merging Vehicles at Junctions Using Mixed-Integer Model Predictive Control," en, in 2018 European Control Conference (ECC), 2018, p. 6.

[Bor04] C. Bordons and E. Camacho, Model predictive control (advanced textbooks in control and signal processing), 2004.

[Con03] D. C. Conner, A. A. Rizzi, and H. Choset, "Composition of local potential functions for global robot control and navigation," in Proceedings 2003 IEEE/RSJ International Conference on Intelligent Robots and Systems (IROS 2003), IEEE, vol. 4, 2003, pp. 3546–3551.

[Fil18] A. Filotheou, A. Nikou, and D. V. Dimarogonas, "Decentralized control of uncertain multi-agent systems with connectivity maintenance and collision avoidance," in 2018 European Control Conference (ECC), IEEE, 2018, pp. 8–13.

[Fuk20] K. Fukuda, "Polyhedral computation,", 2020.

[Gon15] D. González, J. Pérez, V. Milanés, and F. Nashashibi, "A review of motion planning techniques for automated vehicles," IEEE Transactions on intelligent transportation systems, vol. 17, no. 4, pp. 1135–1145, 2015.

[Jan17] F. Janeček, M. Klaučo, M. Kalúz, and M. Kvasnica, "OPTIPLAN: A Matlab Toolbox for Model Predictive Control with Obstacle Avoidance," IFAC-PapersOnLine, 20th IFAC World Congress, vol. 50, no. 1, pp. 531–536, Jul. 2017, ISSN: 2405-8963.

[Jau01] L. Jaulin et al., Interval analysis. Springer, 2001.

References II

[Kar11] S. Karaman and E. Frazzoli, "Sampling-based algorithms for optimal motion planning," en, The International Journal of Robotics Research, vol. 30, no. 7, pp. 846–894, Jun. 2011, ISSN: 0278-3649. (visited on 05/14/2018).

[Kha86] O. Khatib, "Real-time obstacle avoidance for manipulators and mobile robots," in Autonomous robot vehicles, Springer, 1986, pp. 396–404.

[Kod90] D. E. Koditschek and E. Rimon, "Robot navigation functions on manifolds with boundary," Advances in applied mathematics, vol. 11, no. 4, pp. 412–442, 1990.

[LaV06] S. M. LaValle, Planning algorithms. Cambridge university press, 2006.

[Li03] X. R. Li and V. P. Jilkov, "Survey of maneuvering target tracking. part i. dynamic models," IEEE Transactions on aerospace and electronic systems, vol. 39, no. 4, pp. 1333–1364, 2003.

[Lyc18] T. Lyche, C. Manni, and H. Speleers, "Foundations of spline theory: B-splines, spline approximation, and hierarchical refinement," in Splines and PDEs: From Approximation Theory to Numerical Linear Algebra, Springer, 2018, pp. 1–76.

[Mou13] M. A. Mousavi, Z. Heshmati, and B. Moshiri, "Ltv-mpc based path planning of an autonomous vehicle via convex optimization," in 2013 21st Iranian Conference on Electrical Engineering (ICEE), IEEE, 2013, pp. 1–7.

References III

[Nic22] T.-G. Nicu, F. Stoican, and I. Prodan, “Polyhedral potential field constructions for obstacle avoidance in a receding horizon formulation,”, Elsevier, 2022, pp. 254–259. [Online]. Available: https://www.researchgate.net/profile/Florin-Stoican/publication/358248540_Polyhedral_potential_field_constructions_for_obstacle_avoidance_in_a_receding_horizon_formulation/links/627a93b93a23744a7273a09c/Polyhedral-potential-field-constructions-for-obstacle-avoidance-in-a-receding-horizon-formulation.pdf.

[Pal84] S. Pallottino, “Shortest-path methods: Complexity, interrelations and new propositions,” Networks, vol. 14, no. 2, pp. 257–267, 1984.

[Pro16] I. Prodan, F. Stoican, S. Olaru, and S.-I. Niculescu, Mixed-integer representations in control design: Mathematical foundations and applications. Springer, 2016.

[Ric05] A. Richards and J. How, “Mixed-integer programming for control,” in Proceedings of the 2005, American Control Conference, 2005., Jun. 2005, 2676–2683 vol. 4.

[Sto22] F. Stoican, T.-G. Nicu, and I. Prodan, “A mixed-integer mpc with polyhedral potential field cost for collision avoidance,”, Published in ACC’22, 2022, pp. 1–6. DOI: 10.13140/RG.2.2.20230.24643.

[Szm17] M. Szmuk, C. A. Pascucci, D. Dueri, and B. Acikmese, “Convexification and real-time on-board optimization for agile quad-rotor maneuvering and obstacle avoidance,” in 2017 IEEE/RSJ International Conference on Intelligent Robots and Systems (IROS), Sep. 2017.

[Vla18] P. Vlantis, C. Vrohidis, C. P. Bechlioulis, and K. J. Kyriakopoulos, “Robot navigation in complex workspaces using harmonic maps,” in 2018 IEEE International Conference on Robotics and Automation (ICRA), 2018, pp. 1726–1731. DOI: 10.1109/ICRA.2018.8460695.

References IV

[Wei17] A. Weiss, C. Danielson, K. Berntorp, I. Kolmanovsky, and S. D. Cairano, "Motion planning with invariant set trees," in 2017 IEEE Conference on Control Technology and Applications (CCTA), Aug. 2017, pp. 1625–1630.